Am J Transl Res 2020;12(5):1728-1740
www.ajtr.org /ISSN:1943-8141/AJTR0096707

Original Article

The distribution of macrophage subtypes and their relationship to bone morphogenetic protein 2 in calcified aortic valve stenosis

Eiichi Oba[1], Naing Ye Aung[2], Rintaro Ohe[2], Mitsuaki Sadahiro[1], Mitsunori Yamakawa[2]

[1]*Second Department of Surgery,* [2]*Department of Pathological Diagnostics, Yamagata University Faculty of Medicine, Yamagata, Japan*

Received May 8, 2019; Accepted April 14, 2020; Epub May 15, 2020; Published May 30, 2020

Abstract: Activation of the osteogenic signaling cascade (OSC) is thought to be involved in aortic valve stenosis. The aim of this study was to clarify the distribution of macrophage (M) subtypes in the calcified aortic valve and to clarify the relationship between osteoblast-like cells (OLC) and OSC activation. Thirty-six cases of calcified aortic valve were set as the calcification group, and six autopsy cases of aortic valve without pathological calcification comprised the noncalcification group. Aortic valve tissues were used in histological studies including single and double immunostaining to identify M subtypes, bone morphogenetic protein 2 (BMP2) and osteopontin, reverse transcription polymerase chain reaction (RT-PCR) for *CD206*, *heme oxygenase-1* (*HO-1*), and *BMP2* mRNAs and *in situ* RT-PCR for *BMP2* mRNA. Ms positive for CD68, CD163, CD206, and HO-1 were significantly higher in the calcification group than in the noncalcification group ($P < 0.01$). Comparison of the positive cells in each section of the calcification group showed that cells of all M subtypes were found around calcifications. Osteopontin$^+$ cells were also observed around calcifications. CD163$^+$/CD206$^+$ M2 and CD163$^+$/HO-1$^+$ Mox were significantly higher in the sponge layer in both groups. In double immunofluorescence, CD206$^+$ and a portion of HO-1$^+$ Ms expressed BMP2, and in RT-PCR, *CD206* or *HO-1* mRNA was expressed in cases in which BMP2 was expressed. In *in situ* RT-PCR, expression of *BMP2* mRNA was observed around calcifications. This work clarifies the distribution of M subtypes in calcified aortic valves. In addition, the results suggest that CD206$^+$ M2 and HO-1$^+$ Mox, which express BMP2 in calcified aortic valves, are OLC candidates.

Keywords: Aortic valve stenosis, macrophages, M2, Mox, osteoblast-like cell

Introduction

Aortic valve stenosis (AS) is a disease in which ejection of blood from the left ventricle to the aorta is impaired because the aortic valve is subject to opening due to various causes. Until approximately 1980, rheumatic AS due to streptococcal infection in early childhood was considered a possible cause of this condition. Although the incidence of rheumatic AS in developed countries has decreased drastically because the number of cases of rheumatic fever has decreased due to the use of anti-biotics, the number of AS cases due to age-related degeneration of the aortic valve is increasing yearly with the increased elderly population and the advent of dialysis [1, 2].

The most problematic issue in age-related degeneration of the aortic valve is calcification, which markedly reduces valve mobility. Calcification makes it difficult for surgeons to resect the valve leaflets. Consequently, it is necessary to analyze the mechanism of calcification and find preventive or therapeutic methods.

In the calcified aortic valve, the osteogenic signaling cascade (OSC), which involves bone morphogenetic protein 2 (BMP2), a marker of osteoblast-like cells (OLC) and the Wnt/β-catenin signaling cascade, is activated [3, 4]. However, the mechanisms by which the pro-osteogenic signaling cascade is activated are still unknown. Although various types of cells, including myofibroblasts, valvular interstitial cells, and circulating osteoblast lineage cells in the blood (osteoprogenitor cells), have been suggested to be involved in the origin of OLC, the cell types that contribute to it have not yet been definitively identified [5-10].

Changes similar to atherosclerosis are often seen as pathological features of calcified aortic valves [11]. In early lesions, a thickened subendothelial layer, inflammatory cell infiltrations containing many macrophages (Ms) and T lymphocytes, and oxidized lipids are observed. Previous reports have shown that Ms secrete inflammatory cytokines and cause fibrosis, so that the aortic valve is affected by remodeling and calcification [11-14]. In addition, in congenital bicuspid valves, which may undergo AS calcification in younger individuals, Ms are more prevalent than in normal tricuspid valves, suggesting that Ms are likely involved in calcification [15-17]. Furthermore, some altered microRNAs are responsible for the phenotypes of Ms and of valvular interstitial cells in calcified human aortic valves [18-20].

Recent reports classify Ms into five subtypes: M0, M1, M2, Mox, and M4. Although the features of each M subtype have not been fully elucidated, it is believed that M1 causes inflammation and that M2 suppresses differentiation and activation to M1 [21-25]. Mox is also found in oxidized phospholipids and is related to atherosclerosis. M0 is regarded as a precursor cell that differentiates into M1, M2, and Mox. M4 is not derived from M0 but is characterized as expressing the chemokine CXCL4.

At present, the distribution and role of M subtypes in the aortic valve are not fully understood. The aims of this study are to evaluate the distribution of M subsets in calcified aortic valves and to clarify the relationship between OLC and OSC activation.

Materials and methods

Cases

After pathological diagnosis, 36 open heart surgery cases from the Second Department of Surgery (Cardiovascular Surgery), Yamagata University Hospital, Faculty of Medicine, were collected as the AS calcification group [male:female ratio 19:17; average age 76.3 years (57~86 years); bicuspid 9, tricuspid 27; past history: hypertension 29, diabetes mellitus 11, hyperlipidemia 6, hemodialysis 3. Because this study covers only age-related AS, cases of congenital AS and AS suspected to be rheumatic by pathological observation were excluded from this study.

Six autopsy cases without gross or microscopic calcifications in the aortic valve in our institute were used as the noncalcification group (control group) [male:female ratio 5:1; average age 66 years (57~74 years); bicuspid 0, tricuspid 6; past history: hypertension 2, diabetes mellitus 1, hyperlipidemia 2, hemodialysis 0]. The cause of death of all cases was noncardiologic disease.

The isolated aortic valve was immediately divided, fixed in 10% neutral buffered formalin at room temperature for 6~12 hours, embedded in paraffin, and sliced into sections 3 to 5 μm in thickness. The sections were stained with hematoxylin and eosin and elastica-Masson and subjected to immunohistochemistry (IHC), double immunofluorescence (IF) staining, and *in situ* reverse transcription polymerase chain reaction (RT-PCR). In addition, a portion of the isolated aortic valve was frozen in OCT compound in liquid nitrogen, stored at -80°C and used in RT-PCR.

All of the specimens were obtained with the written consent of the patient. This study was approved by the Research Ethics Committee (H24-167) of Yamagata University Faculty of Medicine, Yamagata, Japan.

Immunohistochemistry

IHC was performed using antibodies against CD68 (KP1; mouse IgG1, Dako, Carpinteria, CA, USA), inducible nitric oxide synthase (iNOS) (rabbit polyclonal, Abcam, Cambridge, UK), CD163 (10D6; mouse IgG1, Novocastra, Newcastle upon Tyne, UK), CD206 (5C11; mouse IgG1, Abnova, Taipei, Taiwan), heme oxygenase (HO)-1 (D-8; mouse IgG1, Santa Cruz, Dallas, TX, USA), BMP2 (rabbit, polyclonal, Abcam), and osteopontin (OPN; rabbit polyclonal, Abcam). For IHC, formalin-fixed and paraffin-embedded tissue sections (4 μm in thickness) were blocked with 0.3% H_2O_2 in methanol at 4°C for 30 min and then subjected to antigen retrieval in trypsin for 30 min at 37°C for anti-CD68 antibody, in citric acid (Antigen Retrieval Solution pH 6; Iatron Laboratories Inc., Tokyo, Japan) for anti-CD 163 antibody, anti-iNOS antibody, anti-HO-1 antibody, and anti-OPN antibody, and in EDTA (pH 9.0; Nichirei, Tokyo, Japan) in an autoclave (2 atmospheres, 121°C, 20 min) for anti-CD206 antibody. The sections were incubated with

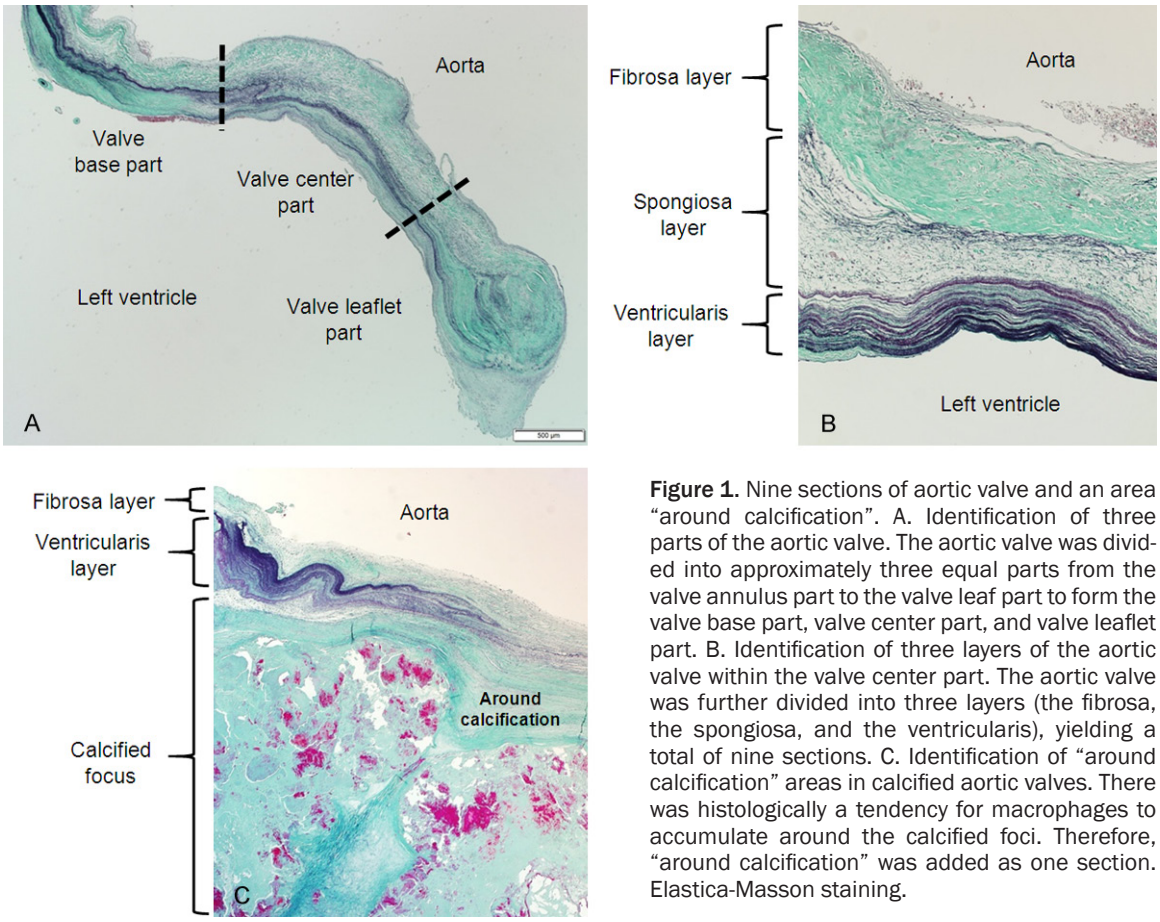

Figure 1. Nine sections of aortic valve and an area "around calcification". A. Identification of three parts of the aortic valve. The aortic valve was divided into approximately three equal parts from the valve annulus part to the valve leaf part to form the valve base part, valve center part, and valve leaflet part. B. Identification of three layers of the aortic valve within the valve center part. The aortic valve was further divided into three layers (the fibrosa, the spongiosa, and the ventricularis), yielding a total of nine sections. C. Identification of "around calcification" areas in calcified aortic valves. There was histologically a tendency for macrophages to accumulate around the calcified foci. Therefore, "around calcification" was added as one section. Elastica-Masson staining.

primary antibodies at room temperature overnight. The labeled streptavidin-biotin peroxidase method (UltraTech HRP Streptavidin-Biotin Detection system, PN IM2391; Immunotech, Marseille, France) was used. A positive reaction was detected as brown color on incubation with 3,3'-diaminobenzidine tetrahydrochloride (Dojindo, Kumamoto, Japan). The sections were then counterstained with hematoxylin. Human tonsil tissue was used as a positive control. Phosphate-buffered saline (0.01 M, pH 7.4) (omitting primary antibody), Universal Negative Control-Mouse (N1698; DAKO) and Universal Negative Control-Rabbit (N1699; DAKO) were used as negative controls. In accordance with Taghavie-Moghadam *et al*. [24], the following markers were used to identify M subtypes: M1 is $CD68^+$, $iNOS^+$, and $CD163^-$; M2 is $CD68^+$, $CD206^+$, and $CD163^+$; and Mox is $CD68^+$, $HO\text{-}1^+$, and $CD163^+$. Because no specific antibodies are available for the detection of M0 and M4 in formalin-fixed and paraffin-embedded tissue sections, they were not identified in this study.

Measurement of positive cells by IHC was conducted as follows. First, each paraffin section was divided into approximately three equal parts from the valve annulus to the valve leaf, creating a valve base part, a valve center part, and a valve leaflet part. Elastica-Masson staining was used to identify the fibrosa, spongiosa, and ventricularis layers of the aortic valve; thus, each section was divided into nine parts (**Figure 1A**, **1B**). In addition, there was a tendency for M to accumulate around calcified foci (**Figure 1C**). Therefore, "around calcification" was added as one section; this section was defined as a region in which immunopositive cells were measured in up to 20 views of high-power-view field (×400) while observing a calcification occupying approximately 20% of one view of the high-power-view field. Each section was observed in up to 20 high-power-view fields (×400). The frequency of cells positive for OPN in areas "around calcification" and areas remote from calcification was compared in six cases with and without calcification, respectively. The frequencies of positive cells in

Table 1. Frequency of calcification in nine valve sections in patients with aortic valve stenosis

Layer	Valve base part	Valve center part	Valve leaflet part
Fibrosa layer	54.6%	65.5%	30.3%
Spongiosa layer	37.0%	47.1%	18.5%
Ventricularis layer	7.6%	12.6%	9.2%

each section were evaluated by two independent observers, and the mean values per high-power-view field are reported.

Double IF staining

Double IF staining of formalin-fixed and paraffin-embedded tissue sections of calcified aortic valves was performed as previously described [26] using antibodies against BMP2, CD68, CD206, and HO-1. In brief, following antigen retrieval, tissue sections were incubated overnight with a cocktail of primary antibodies followed by incubation with fluorescein-conjugated AffiniPure goat anti-rabbit IgG (H+L) (Jackson ImmunoResearch Laboratories, West Grove, PA, USA) for BMP2 detection and with rhodamine-conjugated AffiniPure donkey anti-mouse IgG (H+L) (Jackson ImmunoResearch Laboratories) for identification of M subsets. Because the anti-iNOS antibody and the anti-BMP2 antibody were both rabbit polyclonal antibodies, double IF staining could not be performed. Therefore, single IF staining of serial sections with each antibody was performed. Nuclei were counterstained with DAPI (4',6-diamidino-2-phenylindole). IF was performed to observe the co-expression of BMP2 in M subsets under a fluorescence microscope.

Reverse transcription polymerase chain reaction

RT-PCR was performed using frozen specimens of 10 calcified aortic valves, 5 noncalcified aortic valves, and 1 human tonsil as a positive control. Total messenger RNA (mRNA) was extracted from the frozen specimens and purified; purification included a DNase treatment step using QIA shredder (QIAGEN, Duesseldorf, Germany) and the RNeasy MINI kit (QIAGEN) according to the manufacturer's instructions. Complementary DNA (cDNA) was synthesized using a Reverse Transcription Kit (QIAGEN). The resulting cDNA was used as a template for PCR analysis using Emerald Amp PCR Master Mix (Takara Bio, Otsu, Japan). The forward- and reverse-specific primers, amplicon sizes, and annealing temperatures were as follows: glyceraldehyde-3-phosphate dehydrogenase (GAPDH), 5'-TTGGTATCGTGGAAGGACTC-3' (forward) and 5'-CGCTGTTGAAGTCAGAGGAGAC-3' (reverse), 138 bp, 60°C; CD206, 5'-CACCATCGAGGAATTGGACT-3' (forward) and 5'-ACAATTCGTCATTTGGCTCA-3' (reverse), 62 bp, 60°C [27]; HO-1, 5'-ATGACACCAAGGACCAGAGC-3' (forward) and 5'-GTGTAAGGACCCATCGGAGA-3' (reverse), 153 bp, 55°C [28]; and BMP2, 5'-GACACTGAGACGCTGTTCC-3' (forward) and 5'-CCATGGTCGACCTTTAGG-3' (reverse), 202 bp, 57°C [29]. The PCR products were subjected to electrophoresis in 4% agarose gels (NuSieve 3-1 Agarose; LONZA, Rockland, ME) in 1x TAE buffer solution and visualized by staining with ethidium bromide.

In situ reverse transcription polymerase chain reaction

In situ RT-PCR of BMP2 was performed using paraffin-embedded tissue obtained from calcified aortic valves. The conditions used for IN SITU PCR were as described elsewhere [30]. Briefly, dewaxed and rehydrated 3~5 μm paraffin sections were heated in a thermal cycler at 99°C for 6 sec to block endogenous phosphatase and fixed in 4% paraformaldehyde for 4 hours at room temperature. After fixation, the slides were incubated in proteinase K (DAKO, ready-to-use, #S3020) for 15 min at 37°C. The sections were then heated at 95°C for 2 min to stop protein digestion, air-dried and incubated in DNase digestion solution (DNase I recombinant, RNase-free, Roche Diagnostics, Mannheim, Germany) at 37°C overnight.

After DNase digestion, reverse transcription was performed using the solution provided with the PrimeScript II cDNA synthesis kit (Takara) according to the manufacturer's protocol. Coverslips were placed over the solutions in the DNase digestion and reverse transcriptase reactions to prevent evaporation of the solutions. Slide sealers (Takara) were placed on the slides around the tissue prior to PCR. The IN SITU PCR reaction mix consisted of PCR buffer containing 15 mM $MgCl_2$, PCR digoxigenin (DIG) labeling mix, Taq DNA polymer-

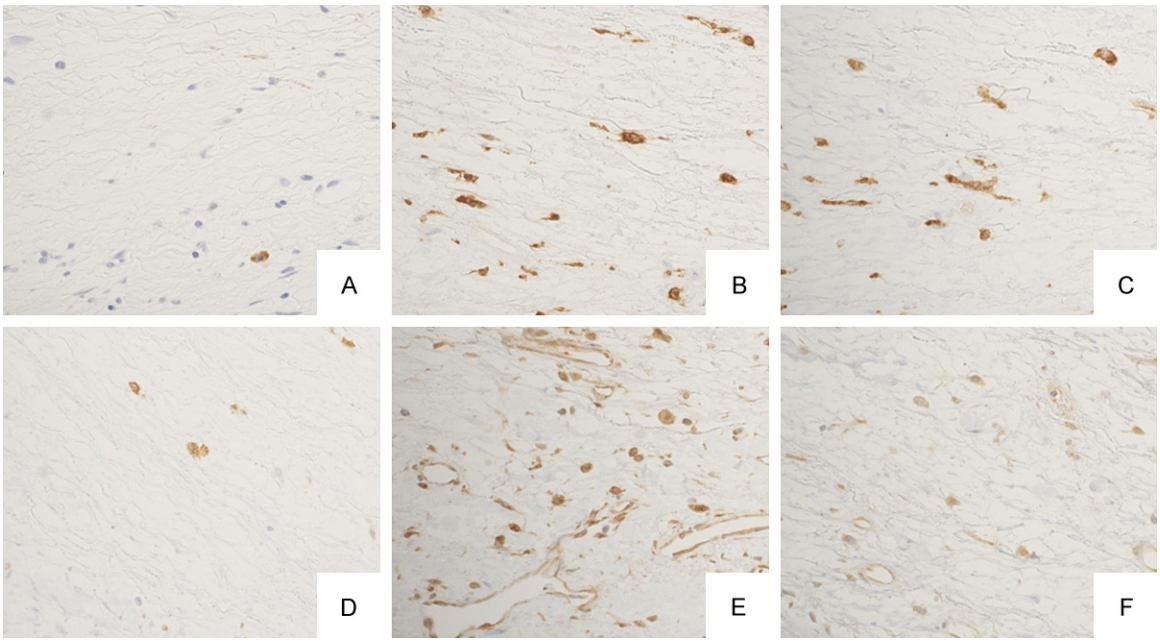

Figure 2. Representative immunostaining images showing the expression of macrophage subtype markers [CD68 (A), CD163 (B), CD206 (C), heme oxygenase-1 (D), and inducible nitric oxide synthase (iNOS) (E)] and bone morphogenetic protein 2 (BMP2) (F) by single immunohistochemistry in the valve center part and spongiosa layer of a single case in the calcification group. Cells of the iNOS$^+$ M1 and CD163$^+$/CD206$^+$ M2 subtypes frequently increased, while cells of the CD68$^+$ M1/M2 subtype and heme oxygenase-1$^+$ Mox subtypes were relatively few. Note that scattered BMP2$^+$ cells were also present. iNOS and BMP2 were present in some vascular endothelial cells.

Table 2. Frequency of cells immunopositive for macrophage subtype markers and bone morphogenetic factor-2 (BMP2) in the calcification and noncalcification groups

Antibody	Number of positive cells/high-power field (×400) (Mean ± SD)	
	Calcification group	Noncalcification group
CD68	0.44 ± 1.35	0.07 ± 0.21
CD163	1.43 ± 2.10	0.86 ± 1.28
iNOS	2.16 ± 4.29	1.38 ± 1.79
CD206	1.03 ± 1.61	0.42 ± 0.74
HO-1	0.47 ± 2.19	0.01 ± 0.05
BMP2	0.88 ± 1.79	absent

SD, standard deviation; iNOS, inducible nitric oxide synthase; HO-1, heme oxygenase-1.

ase and primer pairs for BMP2 (the same primer pairs that were used in RT-PCR). A total of 125 μL of PCR reaction mix was applied to the tissue sections, which were then sealed with slide sealers. The slides were placed in a MasterCycler® PCR thermal cycler (Eppendorf, Hamburg, Germany) for 1 cycle of 94°C for 2 min, 30 cycles of 94°C for 30 sec, 57°C for 30 sec, and 72°C for 45 sec, and 1 cycle of 72°C for 7 min. The location of DIG incorporated into PCR amplicons was detected by an alkaline phosphatase assay using anti-DIG-alkaline phosphatase Fab fragments (1:100 dilution) (Roche Diagnostics), which were incubated with the samples for 30 min at 37°C. The IN SITU PCR product was detected using a Vulcan fast red chromogen kit 2 (Biocare Medical, Concord, CA, USA), and the samples were counterstained with hematoxylin. Tissue sections without primers and without reverse transcriptase reactions were used as negative controls.

Statistical analysis

JMP 10.0.2 software (SAS Institute, Cary, NC, USA) was used for statistical analysis. The Mann-Whitney *U* test was used to compare the number of positive cells in each section in the two groups. In addition, the Steel-Dwass test was performed to compare the number of positive cells in three or more groups. Differences with $P < 0.05$ were considered to be significant.

Table 3. Frequency of cells immunopositive for macrophage subtype markers and bone morphogenetic protein 2 in four parts of the aortic valve in the calcification and noncalcification groups

Antibody/Valve part	Number of positive cells/high-power field (×400) (Mean ± SD)	
	Calcification group (n = 36)	Noncalcification group (n = 6)
CD68		
Valve base part	0.51 ± 0.89	0.13 ± 0.31
Valve center part	0.59 ± 1.91	0.04 ± 0.11
Valve leaflet part	0.21 ± 0.99	0.04 ± 0.13
Around calcification	0.67 ± 1.01	absent
CD163		
Valve base part	1.84 ± 2.48	1.04 ± 1.43
Valve center part	1.63 ± 2.09	0.95 ± 1.15
Valve leaflet part	0.83 ± 1.46	0.59 ± 1.23
Around calcification	2.12 ± 2.18	absent
CD206		
Valve base part	1.25 ± 1.82	0.58 ± 0.91
Valve center part	1.17 ± 1.78	0.48 ± 0.78
Valve leaflet part	0.67 ± 1.07	0.19 ± 0.39
Around calcification	1.97 ± 1.72	absent
Heme oxygenase-1		
Valve base part	0.42 ± 1.28	0.01 ± 0.05
Valve center part	0.66 ± 3.19	0.01 ± 0.06
Valve leaflet part	0.32 ± 1.58	0. ± 0.
Around calcification	0.65 ± 1.00	absent
Inducible nitric oxide synthase		
Valve base part	2.08 ± 3.68	1.56 ± 1.75
Valve center part	2.35 ± 4.33	1.50 ± 2.10
Valve leaflet part	2.03 ± 4.80	1.08 ± 1.46
Around calcification	3.31 ± 4.83	absent
Bone morphogenetic protein 2		
Valve base part	0.99 ± 1.90	0. ± 0.
Valve center part	1.03 ± 1.71	0. ± 0.
Valve leaflet part	0.62 ± 1.72	0. ± 0.
Around calcification	0.98 ± 1.66	absent

SD, standard deviation; Mann-Whitney U test: *, $P < 0.01$: **, $P < 0.05$.

Results

Evaluation of calcification in AS surgical specimens by hematoxylin and eosin staining and elastica-Masson staining

Prior to the measurement of immunopositive cells, each section of the AS surgical specimens was evaluated for calcification. Calcification was more common in the valve base and valve center than in the valve leaflet, more common in the spongiosa layer than in the ventricularis layer, and even more common in the fibrosa layer. Calcification was most commonly (65.5%) found in the fibrosa/valve center (**Table 1**).

Distribution of M subtypes in the calcification and noncalcification groups by IHC

Representative images obtained by single-label immunohistochemistry are shown in **Figure 2**. Among the M subtypes, iNOS$^+$ M1 was the most common in both the calcification and noncalcification groups (**Table 2**). There was no significant difference between the two groups in the frequency of iNOS$^+$ M1 cells. However, the number of cells immunopositive for other M markers (CD68, CD163, CD206, and HO-1) were significantly increased in the AS calcification group compared with the noncalcification group ($P < 0.01$). Very few HO-1$^+$ Mox cells were observed in the noncalcification group.

There were significant differences according to the Steel-Dwass test, as follows: In the calcification group: CD68 vs CD163, iNOS, CD206, and HO-1; CD163 vs CD206 and HO-1; iNOS vs HO-1; CD206 vs HO-1 ($P < 0.01$). In the noncalcification group: CD68 vs CD163, iNOS, CD206, and HO-1; CD163 vs iNOS, CD206, and HO-1; iNOS vs CD206 and HO-1; CD206 vs HO-1 ($P < 0.01$).

There were significant differences according to the Mann-Whitney U test, as follows: CD68, CD163, CD206, HO-1, and BMP2 except iNOS:

Table 4. Frequency of cells immunopositive for macrophage subtype markers and bone morphogenetic protein 2 in four layers in the calcification and noncalcification groups

Antibody/Valve layer	Number of positive cells/high-power field (×400) (Mean ± SD)	
	Calcification group (n = 36)	Noncalcification group (n = 6)
CD68		
Fibrosa layer	0.36 ± 1.33	0.02 ± 0.06
Spongiosa layer	0.66 ± 1.80	0.14 ± 0.30
Ventricularis layer	0.29 ± 0.65	0.05 ± 0.17
Around calcification	0.67 ± 1.01	absent
CD163		
Fibrosa layer	1.03 ± 1.90	0.38 ± 0.73
Spongiosa layer	1.98 ± 2.51	1.48 ± 1.48
Ventricularis layer	1.30 ± 1.70	0.71 ± 1.28
Around calcification	2.12 ± 2.18	absent
CD206		
Fibrosa layer	0.46 ± 0.81	0.09 ± 0.19
Spongiosa layer	1.62 ± 2.03	0.83 ± 0.89
Ventricularis layer	1.00 ± 1.53	0.33 ± 0.76
Around calcification	1.97 ± 1.72	absent
Heme oxygenase-1		
Fibrosa layer	0.49 ± 3.15	0. ± 0.
Spongiosa layer	0.63 ± 1.92	0.02 ± 0.08
Ventricularis layer	0.28 ± 0.84	0. ± 0.
Around calcification	0.65 ± 1.00	absent
Inducible nitric oxide synthase		
Fibrosa layer	1.79 ± 3.73	0.97 ± 1.00
Spongiosa layer	2.42 ± 4.45	2.44 ± 2.42
Ventricularis layer	2.25 ± 4.62	0.73 ± 1.04
Around calcification	3.31 ± 4.83	absent
Bone morphogenetic protein 2		
Fibrosa layer	0.71 ± 1.41	0. ± 0.
Spongiosa layer	1.12 ± 2.180	0. ± 0.
Ventricularis layer	0.81 ± 1.67	0. ± 0.
Around calcification	0.98 ± 1.66	absent

SD, standard deviation; Mann-Whitney U test: *, $P < 0.01$: **, $P < 0.05$.

calcification group vs noncalcification group ($P < 0.01$).

Distribution of M subtypes in each part of the aortic valve in the calcification and noncalcification groups by immunohistochemistry

The distribution of positive cells in the valve base, valve center, valve leaflet, and around calcifications of the calcified valves is summarized in **Table 3**. The number of cells expressing M subtype markers was significantly increased around calcifications. In addition, the number of $CD163^+/CD206^+$ M2 and $HO\text{-}1^+$ Mox cells was significantly decreased at the valve leaflet compared to the valve base and the valve center. However, the number of $iNOS^+$ cells in the different valve sections in the calcification group did not differ significantly.

In the noncalcification group, $CD163^+$ M showed a significant difference between the valve center and the valve leaflet, and $CD206^+$ M2 showed a significant difference between the valve base and the valve leaflet. $BMP2^+$ cells, a marker of OLC, were also present in significantly lower numbers in the valve leaflet than in other parts of the valve in the calcification group.

The distribution of positive cells in the fibrosa, spongiosa, and ventricularis layers and around calcifications is summarized in **Table 4**. The number of cells of any M subtype was significantly increased around calcifications compared to other areas. Among the fibrosa, spongiosa, and ventricularis layers, M subtype marker-positive cells, excluding iNOS, tended to be higher in the spongiosa.

In the noncalcification group, M subtype marker-positive cells, except cells positive for HO-1, were significantly increased in the spongiosa. Very few $HO\text{-}1^+$ cells were observed in any sections of the noncalcification group. $BMP2^+$ cells tended to be in the spongiosa, but there was no significant difference.

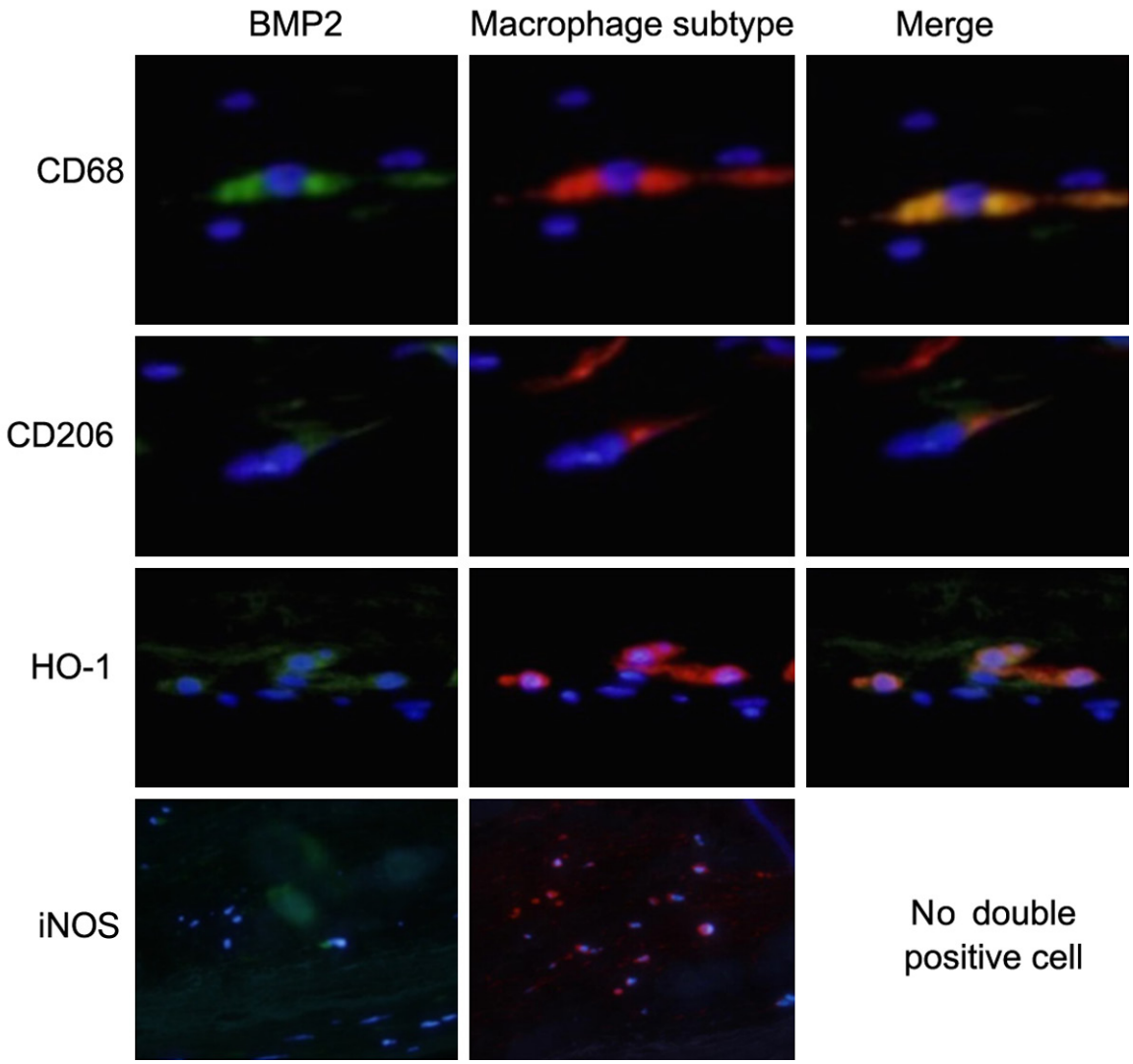

Figure 3. Evaluation of the expression of bone morphogenetic protein 2 (BMP2) in macrophage subtypes by double immunofluorescence staining. Because the anti-iNOS antibody and the anti-BMP2 antibody were both rabbit polyclonal antibodies, single immunofluorescence staining was performed for each of the two proteins using serial sections. Nuclei were counterstained with 4',6-diamidino-2-phenylindole (*blue*). Co-expression of BMP2 (*green*) was confirmed in a subset of the cells that showed positive staining for CD68 (M1/M2 subtype), CD206 (M2 subtype), and heme oxygenase-1 (Mox subtype) (*red*). However, co-expression of iNOS (M1 subtype) and BMP2 was not observed.

Expression of BMP2$^+$ in M subtypes by double IF staining

Co-expression of BMP2 was confirmed in a portion of the cells that were positive for CD68, CD206, and HO-1 (**Figure 3**). Co-expression of iNOS and BMP2 was evaluated in serial sections of 10 specimens but was not observed.

Expression of OPN in six cases with or without calcification by IHC

No OPN expression was observed in a case without calcification (**Figure 4**; **Table 5**). On the other hand, OPN was expressed around calcifications in all cases with calcification. In three cases with calcification, positive cells for OPN were scattered in the area remote from the calcification.

Expression of CD206, HO-1, and BMP2 mRNAs in the aortic valve by reverse transcription polymerase chain reaction

RT-PCR was performed to detect the presence of *CD206*, *HO-1* and *BMP2* mRNAs in tissues of the patients with aortic valve stenosis in the calcification and noncalcification groups.

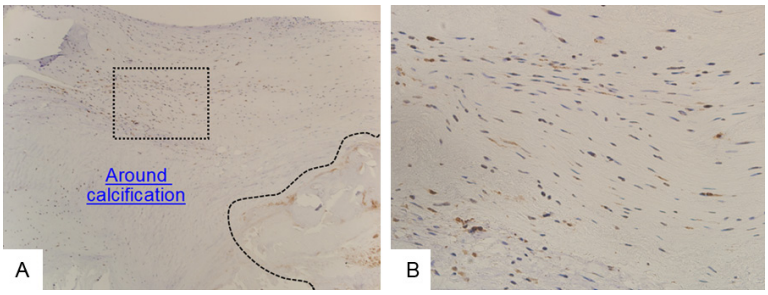

Figure 4. Osteopontin (OPN) immunostaining of calcified aortic valves. (A) OPN was expressed around calcifications in a case with calcification. The calcified focus is encircled by a dotted line. (B) High-power view of the area encircled by the dotted line in (A). Numerous cells positive for OPN were observed around the calcified focus.

Table 5. Frequency of cells immunopositive for osteopontin around calcifications and in areas remote from calcifications

Case number	Calcification	Osteopontin-positive cells	
		Around calcification	In an area remote from calcification
Case 1	Present	+	+
Case 2	Present	+	-/+
Case 3	Present	+	-
Case 4	Present	+	-/+
Case 5	Present	+	-
Case 6	Absent	-	-

-; Negative, -/+; Less frequently positive, +; Frequently positive.

Human tonsil tissue was used as a positive control. GAPDH mRNA (a housekeeping gene) was expressed in all cases. *CD206* mRNA was expressed in 8 cases (80%) in the calcification group and in 3 cases (60%) in the noncalcification group. *HO-1* and *BMP2* mRNAs were expressed in 6 cases (60%) and 5 cases (50%), respectively, in the calcification group and in 4 cases (80%) and 4 cases (80%), respectively, in the noncalcification group (**Figure 5**). In cases in which *BMP2* mRNA was detected, expression of *CD206* and/or *HO-1* mRNA was observed.

Expression of BMP2 mRNA in the aortic valve by in situ reverse transcription polymerase chain reaction

After in situ RT-PCR, *BMP2* mRNA was observed around calcifications of the calcified aortic valve stenosis through Vulcan fast-red staining (**Figure 6**).

Discussion

It has previously been reported that Ms infiltrate the aortic valve from the early stage of AS, and these cells are considered the primary cause of calcification [12, 13]. We investigated the distribution of M subtypes in aortic valve stenosis and the association between BMP2$^+$ cells and calcification, with a special focus on areas around calcifications, using AS surgical specimens.

The immunohistological distribution of M subtypes in the calcification group was compared with that in the noncalcification group. In both groups, M subsets, including iNOS$^+$/CD68$^+$, CD163$^+$/CD206$^+$, and HO-1$^+$ cells, were observed in all sections of the aortic valve. Even in the noncalcification group, M subsets were unexpectedly observed in the aortic valve. In this study, we used six autopsy cases without calcification of the aortic valve as controls (noncalcification group). The average age of the cases was 66 years (57~74 years). The presence of Ms in noncalcified aortic valves may be an age-related phenomenon. iNOS$^+$ M1 were the most frequently observed type of cells in both calcified and noncalcified valves. However, there was no significant difference in the number of iNOS$^+$ M1 cells in calcified and noncalcified valves. In contrast, there were significant differences in CD163$^+$/CD206$^+$ (M2) and HO-1$^+$ (Mox) cells in the calcification and noncalcification groups. This study is the first to demonstrate that HO-1$^+$ Mox are hardly observed in individuals without calcification of the aortic valve. The localization of Mox in atherosclerosis has been reported in some papers [31, 32]. Like atherosclerotic changes, early lesions of AS may begin as a thickening of the subendothelial layer and may be accompanied by the migration and accumulation of all M subsets, including HO-1$^+$ Mox. The increasing colocalization of iNOS$^+$ M1 and CD163$^+$/CD206$^+$ M2 in calcified valves may indicate that the balance between proinflammation (M1) and anti-inflammation (M2) controls the remodeling and calcification of the valve.

In the aortic valve, the valve base and valve center are more mechanically stressed than

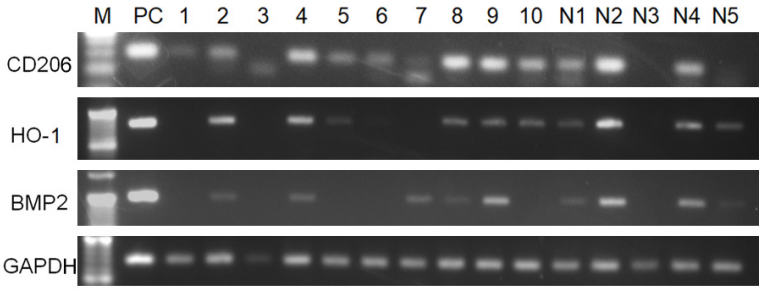

Antibody		Calcified valve										Normal valve				
	PC	1	2	3	4	5	6	7	8	9	10	1	2	3	4	5
CD206	+	-	+	-	+	+	+	+	+	+	+	+	+	-	+	-
HO-1	+	-	+	-	+	+	-	-	+	+	+	+	+	-	+	+
BMP2	+	-	+	-	+	-	-	+	+	+	-	+	+	-	+	+

Figure 5. Evaluation of the expression of *CD206* by cells of the M2 subtype, *heme oxygenase-1* (*HO-1*) by cells of the Mox subtype, and *bone morphogenetic protein 2* (*BMP2*) mRNAs in the aortic valve by reverse transcription polymerase chain reaction. *CD206* mRNA was expressed in 8 cases (80%) in the calcification group and in 3 cases (60%) in the noncalcification group. *HO-1* and *BMP2* mRNAs were expressed in 6 cases (60%) and 5 cases (50%), respectively, in the calcification group and in 4 cases (80%) and 4 cases (80%), respectively, in the noncalcification group. In cells that expressed *BMP2* mRNA, expression of mRNA of *CD206* and/or *HO-1* was observed. Lanes 1-10, calcification group; N1-N5, noncalcification group. M, marker; PC, positive control; GAPDH, glyceraldehyde-3-phosphate dehydrogenase.

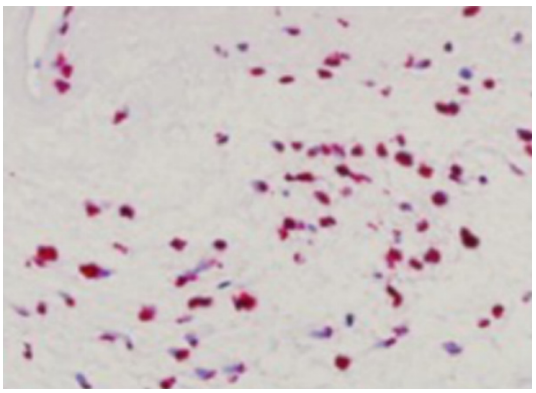

Figure 6. Evaluation of the expression of *bone morphogenetic protein 2* (*BMP2*) mRNA in the aortic valve by *in situ* reverse transcription polymerase chain reaction. Signals for *BMP2* mRNA were observed around calcifications of the calcified aortic valve by Vulcan fast-red staining.

the valve leaflets, often resulting in age-related calcification [33, 34]. In the specimens of the AS calcification group used in this study, calcification was more frequently observed at the valve base and valve center than in the valve leaflet. All the M subtypes were significantly increased in the valve base and valve center in the surrounding calcified areas, suggesting that OSC may be activated at sites where Ms infiltrate and accumulate, leading to the induction of calcification. Furthermore, because significantly fewer BMP2$^+$ cells were found at the valve leaflets, OLC, the origin of OSC, may also be present in the region associated with calcification.

In this study, the results of examination of M subsets in sections of the fibrosa, spongiosa, and ventricularis layers differed somewhat from what was expected. The literature suggests that calcification tends to occur in the fibrosa [35]. In this study, calcification was also found to be more frequent in the fibrosa; we therefore estimated that M are most abundant in the fibrosa. However, significant numbers of M2 and Mox were also observed in the spongiosa. In patients with calcified aortic valve stenosis in an advanced stage requiring operation, most of the fibrosa is occupied by dense acellular fibrosis and calcification, resulting in decreasing M infiltration of this layer. In addition to our finding of the presence of M subsets in the spongiosa of noncalcified aortic valves, it may be suggested that the sponge layer may provide a microvascular network that allows M infiltration.

The association between M subtypes and OLC was evaluated by double IF staining. The results demonstrate for the first time that CD68$^+$ M (all M subtypes), CD206$^+$ M2 and some HO-1$^+$ Mox co-express BMP2; however, iNOS$^+$ M1 did not show co-expression of BMP2. This suggests that activation of OLC involved in mineralization/calcification may occur at least in part due to M2 and Mox.

Expression of OPN in six cases with or without calcification was examined in this study. While no OPN expression was observed in a case

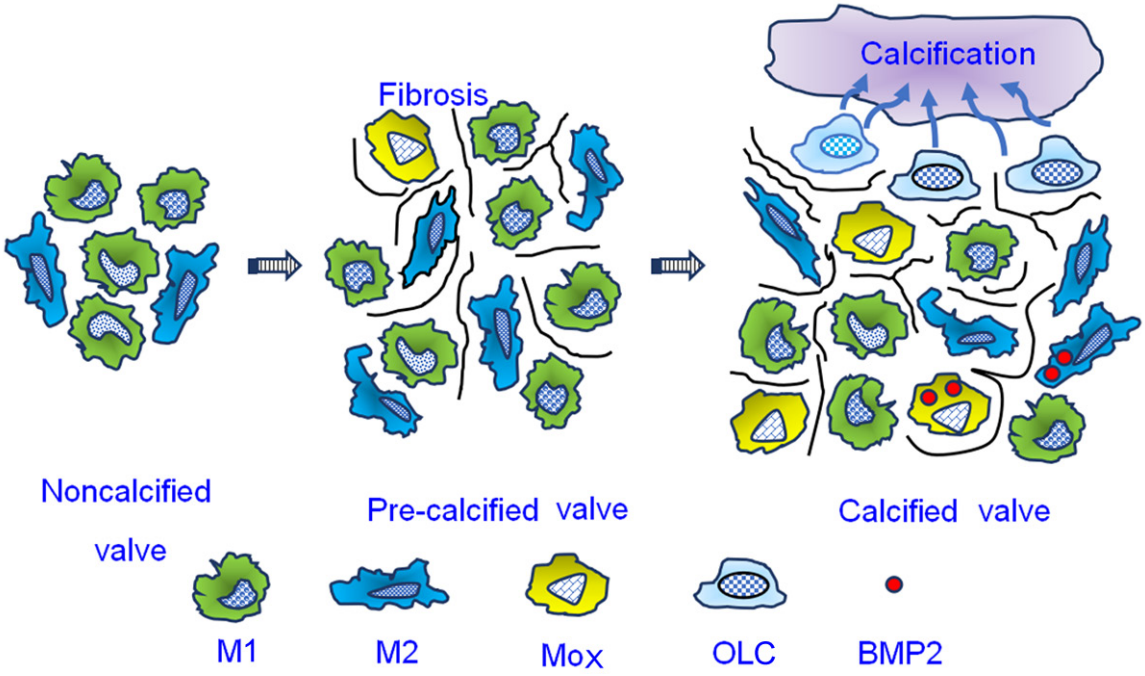

Figure 7. Scheme of a possible mechanism of aortic valve calcification. Noncalcified valves contain a few macrophages, predominantly those of the M1 subtype [inducible nitric oxide synthase (iNOS)$^+$/CD68$^+$] and, less frequently, cells of the M2 subtype (CD68$^+$/CD163$^+$/CD206$^+$). In the pre-calcification phase, against a background of fibrosis, M1 and M2 subtypes gradually accumulate, with a mildly increasing ratio of cells of the M2 subtype to those of the M1 subtype. A few heme oxygenase (HO)-1$^+$ Mox appear. In the calcified valve, calcification is accompanied by the presence of osteoblast-like cells (OLC). In this valve, all subtypes of macrophages are increasing, with a relatively high ratio of cells of the HO-1$^+$ Mox subtype. Some cells of the M2 and Mox subtypes express bone morphogenic protein-2 (BMP2).

without calcification, OPN was expressed around calcifications in all cases with calcification. In three cases with calcification, positive cells for OPN were scattered in areas remote from the calcification. In the adult heart under physiological conditions, basal levels of OPN are expressed. Increased expression of OPN has been correlated with the progression of cardiac remodeling and fibrosis to heart failure and with the severity of the condition [36]. Importantly, OPN isoforms are differentially expressed during calcific aortic valve disease progression and function to inhibit biomineralization, but only when phosphorylated [37, 38]. The effects of OPN on macrophage polarization remain controversial; however, one recent study reported that CD206$^+$ macrophages strongly express OPN and suggested that specific macrophage subtypes involved in tissue repair may differentially express OPN [39]. In the present study, CD206$^+$ macrophages were absent from noncalcified valves, but they were frequently observed in many regions, including areas around calcifications, suggesting that they may have properties similar to those of OPN-expressing cells.

The levels of *CD206*, *HO-1*, and *BMP2* mRNAs in calcified and noncalcified valves were examined by RT-PCR. *BMP2* mRNA was observed in cases in which *CD206* and/or *HO-1* mRNAs were expressed. Furthermore, IN SITU PCR indicated the presence of *BMP2* mRNA around calcifications of calcified aortic valves.

Through this study, we clarified the following for the first time. (1) iNOS$^+$ M1 is the most highly distributed cell subtype in both calcified and noncalcified valves. (2) CD163$^+$/CD206$^+$ M2 and HO-1$^+$ Mox are significantly increased in calcified valves. (3) Some CD206$^+$ M2 and HO-1$^+$ Mox co-express BMP2. (4) BMP2 mRNA was expressed in cases in which CD206 and/or HO-1 mRNA were present. (5) BMP2 mRNA was observed around calcifications of calcified aortic valves through IN SITU PCR. These results suggest that M2 and some Mox cells may be candidates for OLC related to calcification.

Based on our results, we propose the following mechanism of age-related mineralization/calcification of the aortic valve (**Figure 7**). First, mechanical stress is applied, mild inflammation occurs in the aortic valve, and M1 cells migrate. As inflammation progresses, the number of M2 cells increases, suppressing differentiation and activation to M1; Mox cells migrate, and oxidized lipid deposition occurs. Some M2 and Mox cells may have the character of $BMP2^+$ OLC; finally, OSC begins, causing calcification.

As a result of this mechanism, BMP2 is co-expressed by a subset of M2 and Mox cells. Investigation of the difference between M2 and Mox cells that do not co-express BMP2 should further clarify the mechanism through which calcification occurs.

Acknowledgements

This work was supported by a Grant-in-Aid for Scientific Research (C) (17K08736) in Japan. The authors thank Mr. Hitoshi Suzuki, Mrs. Kumiko Abe, Mrs. Junko Takeda, and Mrs. Hiromi Murata of the Department of Diagnostic Pathology, Yamagata University Faculty of Medicine, for their technical support.

Disclosure of conflict of interest

None.

Address correspondence to: Mitsunori Yamakawa, Department of Pathological Diagnostics, Yamagata University Faculty of Medicine, 2-2-2 Iida-Nishi, Yamagata 990-9585, Japan. Tel: +81-23-628-5237; Fax: +81-23-628-5240; E-mail: myamakaw@med.id.yamagata-u.ac.jp

References

[1] Iung B and Vahanian A. Epidemiology of acquired valvular heart disease. Can J Cardiol 2014; 30: 962-970.

[2] Dutta P and Lincoln J. Calcific aortic valve disease: a developmental biology perspective. Curr Cardiol Rep 2018; 20: 21.

[3] Rajamannan NM. Calcific aortic stenosis: lessons learned from experimental and clinical studies. Arterioscler Thromb Vasc Biol 2009; 29: 162-168.

[4] Hakuno D, Kimura N, Yoshioka M and Fukuda K. Molecular mechanisms underlying the onset of degenerative aortic valve disease. J Mol Med (Berl) 2009; 87: 17-24.

[5] Miller JD, Weiss RM and Heistad DD. Calcific aortic valve stenosis: methods, models, and mechanisms. Circ Res 2011; 108: 1392-1412.

[6] Undale A, Srinivasan B, Drake M, McCready L, Atkinson E, Peterson J, Riggs BL, Amin S, Modder UI and Khosla S. Circulating osteogenic cells: characterization and relationship to rates of bone loss in postmenopausal women. Bone 2010; 47: 83-92.

[7] Cho KI, Sakuma I, Sohn IS, Jo SH and Koh KK. Inflammatory and metabolic mechanisms underlying the calcific aortic valve disease. Atherosclerosis 2018; 277: 60-65.

[8] Menon V and Lincoln J. The genetic regulation of aortic valve development and calcific disease. Front Cardiovasc Med 2018; 5: 162.

[9] Näpänkangas J, Ohtonen P, Ohukainen P, Weisell J, Väisänen T, Peltonen T, Taskinen P and Rysä J. Increased mesenchymal podoplanin expression is associated with calcification in aortic valves. Cardiovasc Pathol 2019; 39: 30-37.

[10] Perbellini F, Watson SA, Bardi I and Terracciano CM. Heterocellularity and cellular cross-talk in the cardiovascular system. Front Cardiovasc Med 2018; 5: 143.

[11] Taghavie-Moghadam P, Butcher MJ and Galkina EV. The dynamic lives of macrophage and dendritic cell subsets in atherosclerosis. Ann N Y Acad Sci 2014; 1319: 19-37.

[12] Yetkin E and Waltenberger J. Molecular and cellular mechanisms of aortic stenosis. Int J Cardiol 2009; 135: 4-13.

[13] New SE and Aikawa E. Molecular imaging insights into early inflammatory stages of atrial and aortic valve calcification. Circ Res 2011; 108: 1381-1391.

[14] Li G, Qiao W, Zhang W, Li F, Shi J and Dong N. The shift of macrophages toward M1 phenotype promotes aortic valvular calcification. J Thorac Cardiovasc Surg 2017; 153: 1318-1327.

[15] Moreno PR, Astudillo L, Elmariah S, Purushothaman KR, Purushothaman M, Lento PA, Sharma SK, Fuster V and Adams DH. Increased macrophage infiltration and neovascularization in congenital bicuspid aortic valve stenosis. J Thorac Cardiovasc Surg 2011; 142: 895-901.

[16] Wang R, Chen W, Ma Z, Li L and Chen X. M1/M2 macrophages and associated mechanisms in congenital bicuspid aortic valve stenosis. Exp Ther Med 2014; 7: 935-940.

[17] Akahori H, Tsujino T, Naito Y, Yoshida C, Lee-Kawabata M, Ohyanagi M, Mitsuno M, Miyamoto Y, Daimon T and Masuyama T. Intraleaflet haemorrhage as a mechanism of rapid progression of stenosis in bicuspid aortic valve. Int J Cardiol 2013; 167: 514-518.

[18] Li XF, Wang Y, Zheng DD, Xu HX, Wang T, Pan M, Shi JH and Zhu JH. M1 macrophages promote aortic valve calcification mediated by microRNA-214/TWIST1 pathway in valvular interstitial cells. Am J Transl Res 2016; 8: 5773-5783.
[19] Lu P, Yin B and Liu L. MicroRNA-138 suppresses osteoblastic differentiation of valvular interstitial cells in degenerative calcific aortic valve disease. Int Heart J 2019; 60: 136-144.
[20] Song R, Fullerton DA, Ao L, Zhao KS, Reece TB, Cleveland JC Jr and Meng X. Altered microRNA expression is responsible for the pro-osteogenic phenotype of interstitial cells in calcified human aorticvalves. J Am Heart Assoc 2017; 6.
[21] Rath M, Müller I, Kropf P, Closs EI and Munder M. Metabolism via arginase or nitric oxide synthase: two competing arginine pathways in macrophages. Front Immunol 2014; 5: 532.
[22] Shapouri-Moghaddam A, Mohammadian S, Vazini H, Taghadosi M, Esmaeili SA, Mardani F, Seifi B, Mohammadi A, Afshari JT and Sahebkar A. Macrophage plasticity, polarization, and function in health and disease. J Cell Physiol 2018; 233: 6425-6440.
[23] Gleissner CA. Macrophage phenotype modulation by CXCL4 in atherosclerosis. Front Physiol 2012; 3: 1
[24] Taghavie-Moghadam PL, Butcher MJ and Galkina EV. The dynamic lives of macrophage and dendritic cell subsets in atherosclerosis. Ann N Y Acad Sci 2014; 1319: 19-37.
[25] Kadl A, Meher AK, Sharma PR, Lee MY, Doran AC, Johnstone SR, Elliott MR, Gruber F, Han J, Chen W, Kensler T, Ravichandran KS, Isakson BE, Wamhoff BR and Leitinger N. Identification of a novel macrophage phenotype that develops in response to atherogenic phospholipids via Nrf2. Circ Res 2010; 107: 737-746.
[26] Robertson D, Savage K, Reis-Filho JS and Isacke CM. Multiple immunofluorescence labelling of formalin-fixed paraffin-embedded (FFPE) tissue. BMC Cell Biol 2008; 9: 13.
[27] Ploeger DT, van Putten SM, Koerts JA, van Luyn MJ and Harmsen MC. Human macrophages primed with angiogenic factors show dynamic plasticity, irrespective of extracellular matrix components. Immunobiology 2012; 217: 299-306.
[28] Lim DH, Jang J, Kim S, Kang T, Lee K and Choi IH. The effects of sub-lethal concentrations of silver nanoparticles on inflammatory and stress genes in human macrophages using cDNA microarray analysis. Biomaterials 2012; 33: 4690-4699.
[29] Graham TR, Agrawal KC and Abdel-Mageed AB. Independent and cooperative roles of tumor necrosis factor-, nuclear factor-B, and bone morphogenetic protein-2 in regulation of metastasis and osteomimicry of prostate cancer cells and differentiation and mineralization of MC3T3-E1 osteoblast-like cells. Cancer Sci 2010; 101: 103-111.
[30] Bagasra O. Protocols for the in situ PCR - amplification and detection of mRNA and DNA sequences. Nat Protoc 2007; 2: 2782-2795.
[31] Adamson S and Leitinger N. Phenotypic modulation of macrophages in response to plaque lipids. Curr Opin Lipidol 2011; 22: 335-342.
[32] Bobryshev YV, Ivanova EA, Chistiakov DA, Nikiforov NG and Orekhov AN. Macrophages and their role in atherosclerosis: pathophysiology and transcriptome analysis. Biomed Res Int 2016; 2016: 9582430.
[33] Weiler M, Yap CH, Balachandran K, Padala M and Yoganathan AP. Regional analysis of dynamic deformation characteristics of native aortic valve leaflets. J Biomech 2011; 44: 1459-1465.
[34] Lindman BR, Clavel MA, Mathieu P, Iung B, Lancellotti P, Otto CM and Pibarot P. Calcific aortic stenosis. Nat Rev Dis Primers 2016; 2: 16006.
[35] Togashi M, Tamura K, Masuda Y and Fukuda Y. Comparative study of calcified changes in aortic valvular diseases. J Nippon Med Sch 2008; 75: 138-145.
[36] Abdelaziz Mohamed I, Gadeau AP, Hasan A, Abdulrahman N and Mraiche F. Osteopontin: a promising therapeutic target in cardiac fibrosis. Cells 2019; 8.
[37] Grau JB, Poggio P, Sainger R, Vernick WJ, Seefried WF, Branchetti E, Field BC, Bavaria JE, Acker MA and Ferrari G. Analysis of osteopontin levels for the identification of asymptomatic patients with calcific aortic valve disease. Ann Thorac Surg 2012; 93: 79-86.
[38] Lok ZSY and Lyle AN. Osteopontin in vascular disease. Arterioscler Thromb Vasc Biol 2019; 39: 613-622.
[39] Shirakawa K, Endo J, Kataoka M, Katsumata Y, Yoshida N, Yamamoto T, Isobe S, Moriyama H, Goto S, Kitakata H, Hiraide T, Fukuda K and Sano M. IL (Interleukin)-10-STAT3-Galectin-3 axis is essential for osteopontin-producing reparative macrophage polarization after myocardial infarction. Circulation 2018; 138: 2021-2035.